THE TRIASSIC ALKALINE DOLERITES OF THE VALACLOCHE-CAMARENA AREA (SE-IBERIAN CHAIN, TERUEL): GEODYNAMIC IMPLICATIONS

M. Lago San José *, C. Galé Bornao *, E. Arranz Yagüe *, A. Gil Imaz *
A. Pocovi Juan * y R. Vaquer Navarro **

ABSTRACT

The dolerite sills outcropping in the Valacloche-Camarena area (SE Iberian Chain), are the expression of an alkaline magmatism, emplaced in Keuper facies sedimentary rocks. Their pre-Hettangian age is deduced from the development of fluidality structures at the top of the sills together with the very low grade contact metamorphism of the host rocks. A differentiation trend, represented by two rock-types, with variable Ti-augite content, is confirmed by geochemical data (REE). The alkaline composition of this magmatism is close to that of the OIB type. Crust-derived enclaves (metapelites and granitoids) are common in these sills, suggesting that magma ascent took place through a fracture system, related to a distensive tectonic regime, that affected different levels of the crust. This magmatism was one of the expressions of the triassic rifting events that are well represented in the SE border of the Iberian Chain.

Key words: *dolerites, triassic rifting, enclaves, Iberian Chain.*

RESUMEN

Un magmatismo alcalino, emplazado en sedimentos triásicos en facies Keuper, está bien representado en los sills doleríticos del área de Valacloche-Camarena (SE de la Cordillera Ibérica). La edad pre-Hettangiense ha sido deducida a partir de la presencia de estructuras de fluidalidad y de un metamorfismo de contacto de grado muy débil. Petrológicamente se identifica una fraccionación según dos litotipos (con contenido variable en Ti-augita) que está corroborada por los datos de composición geoquímica (en tierras raras); la composición alcalina de este magmatismo es próxima a la del tipo OIB. La presencia, frecuente, de enclaves de corteza (metapelitas y granitoides) indica una fracturación que, en condiciones distensivas, afectó a distintos niveles de dicha corteza. Este magmatismo está ligado al rifting triásico que está bien expresado en el borde SE de la Cordillera Ibérica.

Palabras clave: *doleritas, rifting triásico, enclaves, Cordillera Ibérica.*

Introduction

Dolerite sills, emplaced in Keuper facies sedimentary rocks in the SE sector of the Iberian Chain (fig. 1) are the expression of a Triassic magmatism, postdated by the Imón Fm. (pre-Hettangian age; Goy & Yébenes, 1977). Preliminary petrological and geochemical data on this magmatism were obtained by Lago *et al.* (1996), showing its differences when compared with a coeval tholeiitic magmatism outcropping in the Valencia area (described in Lago *et al.*, 1999).

This triassic magmatism is exposed in more than a hundred outcrops within seven big diapiric units in this part of the Iberian Chain: Villel, Valacloche-Camarena, Sarrión, Albentosa-Santa Cruz de Moya, San Agustin-Vall de Uxó, Torás and Altura (fig. 1b). As exposed in Lago *et al.* (1996), the main features of this magmatism are:

---

* Departamento de Ciencias de la Tierra. Universidad de Zaragoza. 50009 Zaragoza.
** Departament de Geoquimica, Petrologia i Prospecció Geològica. Universitat de Barcelona. 08071 Barcelona.
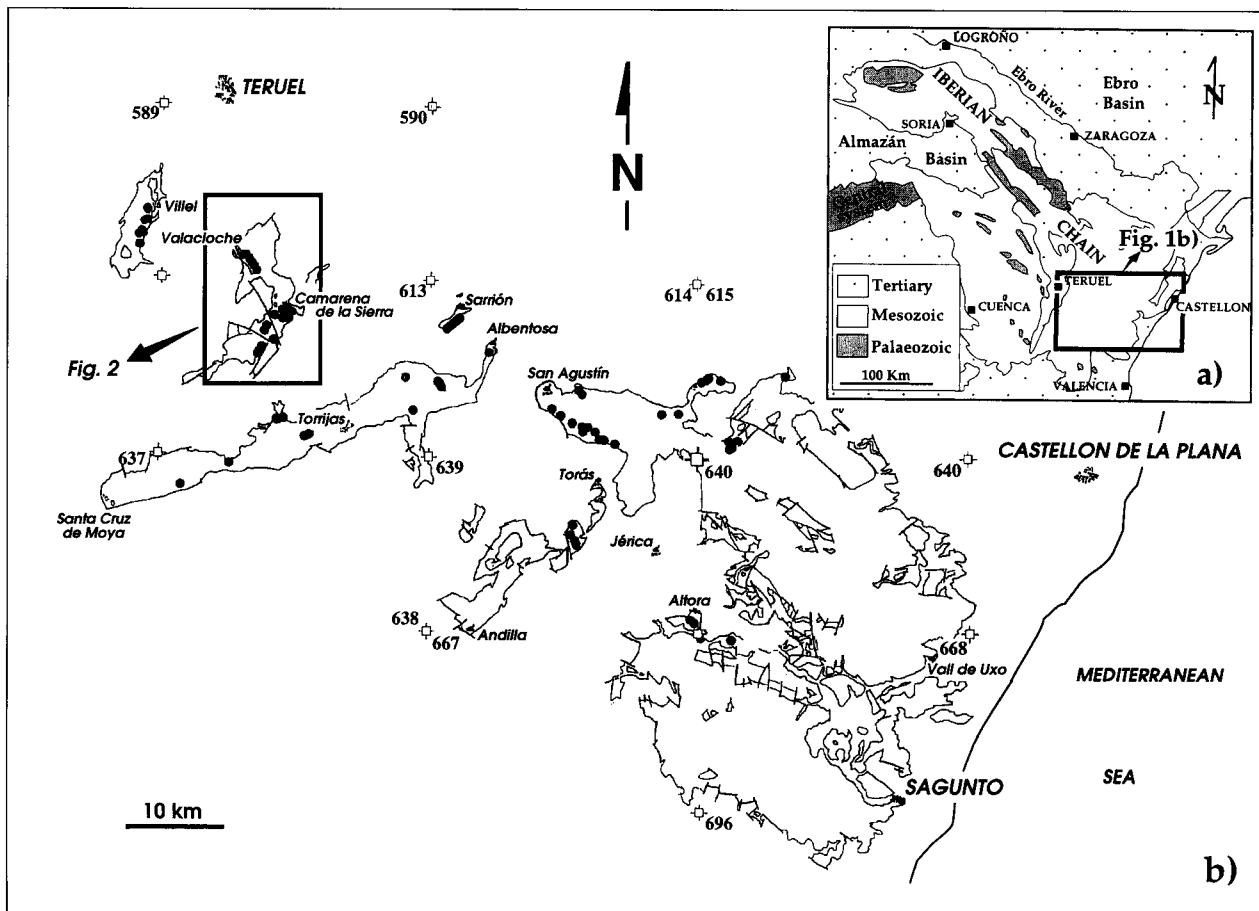
Fig. 1.—Geological setting of studied outcrops (b) in the SE sector of Iberian Chain (a). Detail of the studied area.

(1)   Dolerite intrusions display a lenticular shape, with a thickened central mass, the intrusions in the Camarena area (figs. 1b, 2 and 3b) being the most representative example.

(2)   These sills are emplaced close to the top of the Keuper facies plastic rocks (K1 to K4, according to Ortí, 1990) or, less commonly, within older materials (e.g., Buntsandstein facies, in Pina de Montalgrao and to the E of Albentosa, fig. 1b). In all cases, dolerite sills are emplaced below the dolomitic levels of the Imón Fm., which represents a pre-Hettangian age, according to Goy & Yébenes (1977). Neither explosive terms nor aerial lava flows outcrop.

(3)   The alkaline affinity of this magmatism, expressed by high Nb, Y and P contents, agrees with its mineral composition (Ti-augite, K-rich plagioclase, apatite, titanite and Ti-magnetite).

The Valacloche-Camarena outcrop (figs. 1b and 2) is the most interesting example of this magmatism, because it shows well preserved emplacement structures (fig. 4) and a very low-grade contact metamorphism in the host rocks, allowing us

to propose an emplacement age. On the other hand, crustal enclaves are common in this outcrop (fig. 3b) whereas they are less abundant or totally absent in others. Taking into account all this data, together with its age and composition, this magmatism can be related to the rifting events that affected the SE margin of the Iberian Chain during Triassic times [Salas & Casas (1993); Martínez et al. (1997)].

In this paper we deal with a petrological and geochemical characterization of the dolerites, an interpretation of their emplacement conditions, which allow for an age proposal and finally, we discuss the petrogenetic meaning of this magmatism within the geodynamical context of the Triassic rifting of the SE border the Iberian Chain. The detailed study (mineral and geochemical composition) of crustal enclaves included in the dolerites (figs. 2, 3b, 4A, 4D, 4E and 4F) is another aim of this paper; some previous studies on these enclaves were carried out by Sánchez Cela (1981 and 1982) and Sánchez Cela et al. (1984, and 1987-1988).
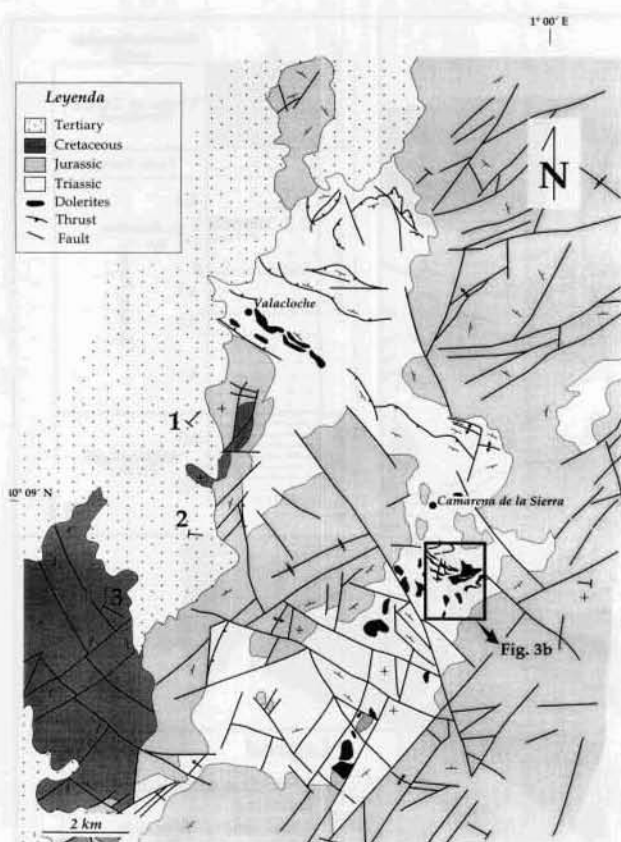
Fig. 2.—Geological sketch map of the Valacloche-Camarena de la Sierra diapiric outcrop.

Age and emplacement conditions

The emplacement age of the alkaline doleritic rocks exposed in the Valacloche-Camarena diapiric outcrop (fig. 2) is well constrained, as they are interbedded within Keuper facies materials (K4 of Ortí, 1990) and the dolomitic Imón Fm. rocks (pre-Hettangian age) overlie both sedimentary and igneous rocks. So, the emplacement age can be placed between Norian and Rhaetian (fig. 3a).

Emplacement conditions can be inferred from two main features. First, the fluidality structures exposed at the upper contact of the sills in Valacloche (fig. 2) and some of the examples to the S of Camarena (figs. 2a and 3b). The most common fluidality structures display ropy (fig. 4C), bulbous or lobate (fig. 4B) developments whick are indicative of a magma movement into the loosely consolidated evaporitic and marly-clayey sediments of the K4 unit. The lateral movement of this low-viscosity magma, acting as a wedge, was favoured by the small load-pressure of the overlying sediments and also by the lower viscosity of the unconsolidated sediment with respect to the intruding magma. In

second place, the very low grade contact metamorphism, that affects only a thin sheet of the host rock suggests a fast cooling process, related to near surface intrusion of the doleritic magma.

The intrusion that outcrops to the south of Camarena (figs. 2 and 3b) shows concordant sheet-like injections in the plastic sediments of the K4 unit that, at a map-scale, are configured as sills with variable thickness between 3 and 150 m. In the Valacloche area (fig. 2) two sills were mapped and studied, with an almost constant thickness (15-25 m) and a wide lateral extension. Two rock-types, indicative of two differentiation stages, were identified in both intrusions: a Ti-augite rich, biotite-poor dolerite, which is the main type in the Valacloche sills and a more differentiated biotite rich dolerite (with scarce Ti-augite crystals) which, in contrast, is the best exposed rock-type in Camarena, where it contains an anomalous accumulation of crustal enclaves (quartzitic, metapelites and rare granitoids; fig. 3b, details in figs. 4A, 4D, and 4F), that represent different levels of the post-variscan crust.

Thus, the emplacement model for this magmatism must consider two successive stages, very close in time, with and without crustal enclaves. The small volume of the sills —as shown in a geological map— suggests small magmatic chambers. Interpretation of spatial relationships between the intrusions and the host rocks and also amongst the two dolerite types and crustal enclaves, allow us to propose that in a first stage, the unevolved liquid, with low water content, would reach its emplacement level within loosely consolidated sediments, under an extensional tectonic regime that favoured pervasive fracturing of crustal rocks in the magma path. The second, more fractionated and more viscous liquid, with a higher water content would have been extruded later, carrying most of the enclaves ripped from different crustal levels. The reaction textures observed in some of the enclaves (granitoids and metapelites) with the host dolerite are explained by their longer contact with the magma. Both stages probably represent the beginning of the Triassic-Jurassic rifting in the SE of the Iberian Chain, characterized by an incipient fracturation in the uppermost part of crust.

In orden to reconstruct the general geometry of the Valacloche-Camarena intrusion three interpretative cross-sections have been made (fig. 5). The main intrusion to the S of Camarena (2-2') is characterized by its lenticular shape and concordant sheet-like injections in Keuper facies rocks. To the NW and to the S of the main outcrop (1 and 3) the intrusions display sill-like sections. The current structure of the area is the result of Alpine deformation stages to which several inverse faults and folds
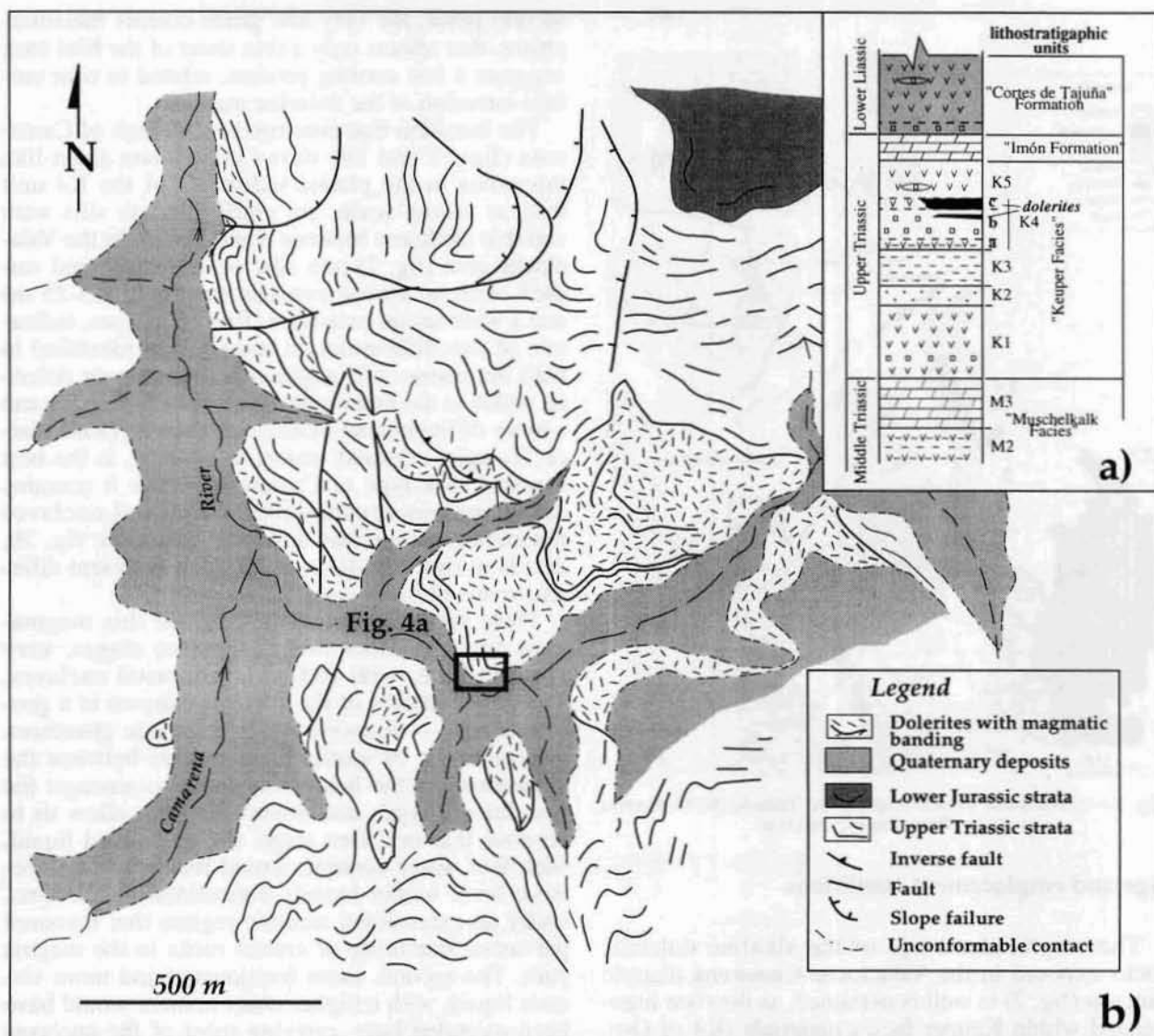
Fig. 3.—Stratigraphic position of dolerites (a) and geological map of Camarena sector (b) indicating the location of the enclave-rich unit.

affecting Muschelkalk facies rocks and also, the verticalization of the Jurassic series in the foot wall of the main thrust (figs. 2 and 3) should be related.

Petrology of enclaves

Enclaves in the Camarena intrusion (figs. 2 and 3b) are accumulated in a 5 m thick, NNW-SSE trending unit (figs. 3b and 4A). This unit is quite homogeneous, as a result of the non-structured and poorly classifed spatial distribution of enclaves, embedded in a differentiated dolerite which acts as a matrix. The sharp contacts of the unit with the

host dolerite are flanked with strongly altered dolerite bands. The largest enclaves are accumulated in the center of the unit whilst the small ones tend to be placed in the borders. In some parts of the unit, a roughly defined orientation of enclaves is observed. Enclaves show angular shapes (figs. 4E and 4F), related to fragmentation and fast transport with little or no reactional textures with the hosting dolerite. These can be grouped into four types:

(1)   Sedimentary: fragments of sedimentary material (pelites) with irregular morphology and size (cm). Their corroded margins and diffuse shapes suggest a partial assimilation in the magma. Anhedral pyroxene (0.2 mm) and accessory epidote —pistaci-
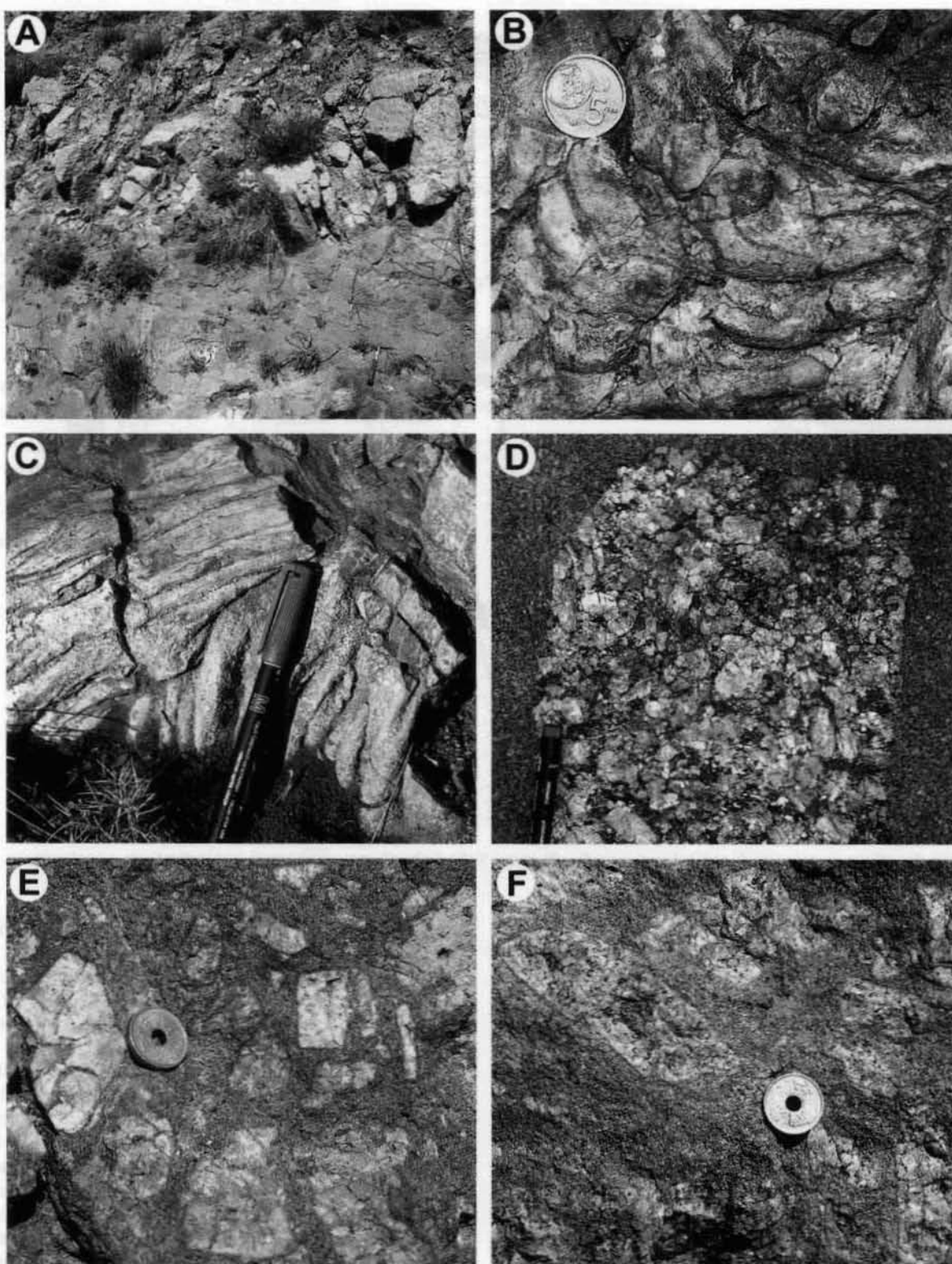
Fig. 4.—(A): Contact between pyroxene-rich and biotite-rich dolerites. The latter includes crustal enclaves. (B and C): Fluidality structures at the top of the Valacloche sill, bulbous type (B) and ropy type (C). In (D): Detail of a granitoid enclave in pyroxene rich dolerite. (E and F): Quartzite enclaves embedded in biotite-rich dolerite, showing thin pyroxene rims.
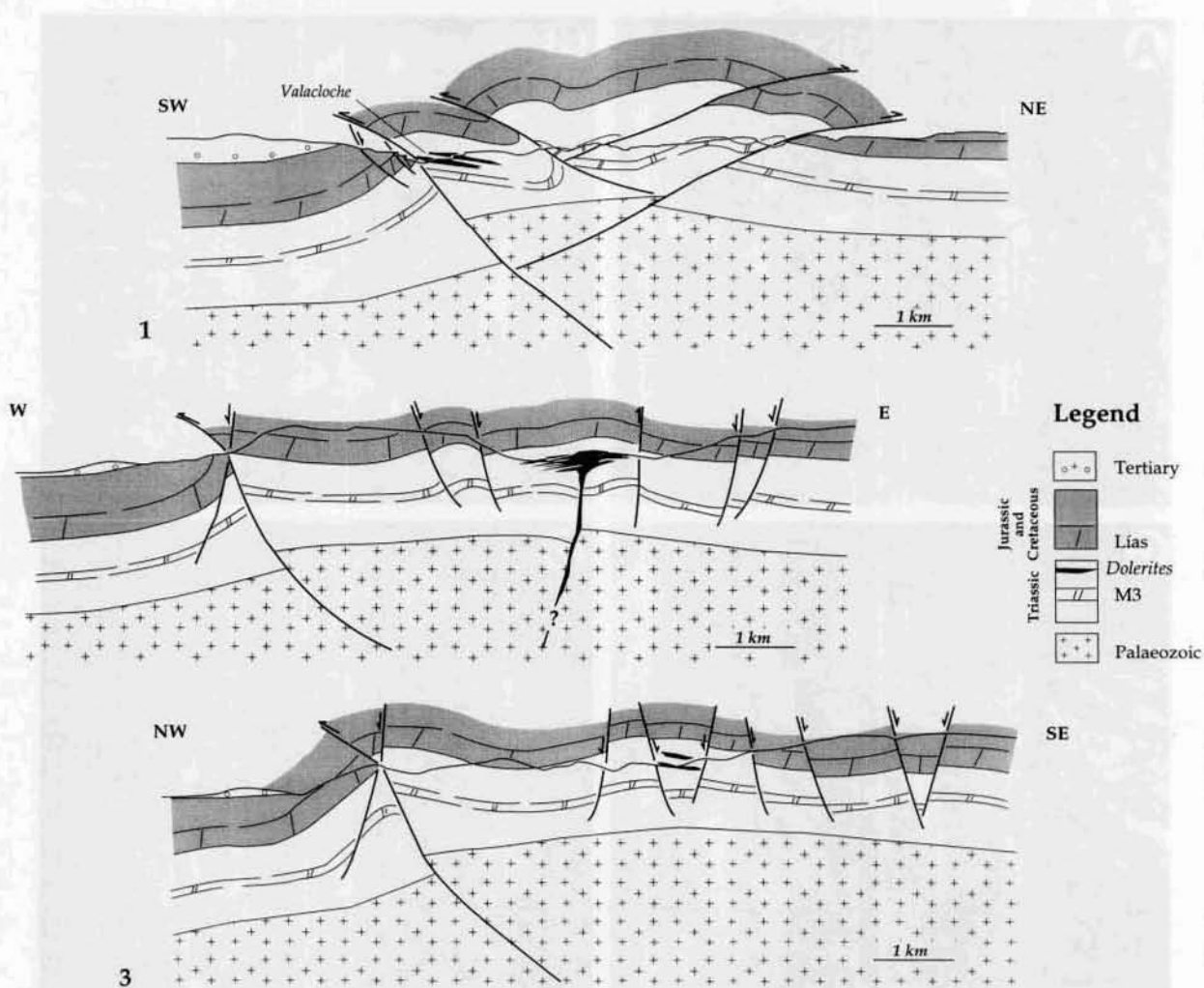
Fig. 5.—Cross sections (1, 2 and 3: location in fig. 2) of the Valacloche-Camarena diapir (see text for further explanation).

te— (0.8 mm) and chlorite (0.4 mm) crystals are common in the reaction margin around the enclaves.

(2)   Quartzitic: these are the most common enclaves (90 %); they are heterometric in size (dm) and angular in shape (figs. 4E and 4F). Their contact with the dolerite is generally sharp, with no evidence of reaction or resorption by the magma. Some of the enclaves show clinopyroxene rims (2.5 mm thickness on average). Clinopyroxene crystals in these rims (figs. 4E and 4F; composition in figs. 7a, b and c, and analysis 9 to 12 in table 1) grew radially on the surface of the enclave, which acted as a crystallization nucleus.

(3)   Igneous: granitoid and aplite enclaves are quite common, displaying sharp contacts, with little or no reaction with the dolerite (fig. 4D). Granitoids have porphyritic-hypidiomorphic textures and their mineral association is composed of altered plagio-

clase (25 %; An$_{40-35}$ as shown in table 3), potassium feldspar (40-45 %) and quartz (30-35 %).

(4)   High grade metapelites: the most common type consists of quartz (30-35 %), alkali feldspar (30-35 %) and altered plagioclase as the main components. Sillimanite (5-10 %) is frequent both as the fibrous variety (fibrolite) and idioblastic prisms, surrounded occasionally by potassium feldspar relics. Anhedral spinel (hercinite; $mg^* = 0.31\text{-}0.32$; table 7), rutile and anhedral amphibole (Mg-hornblende and actinolite; table 5) are accessory phases. Some enclaves contain associations of small (0.1 mm) anhedral garnet crystals or in other samples, the mineral association is composed of spinel (table 7) included in cordierite (table 9) together with prismatic sillimanite (table 8), biotite (analysis 7 to 10 in table 2), Ti-magnetite (table 10) and potassium feldspar. Most of these enclaves show sharp boundaries and reactional
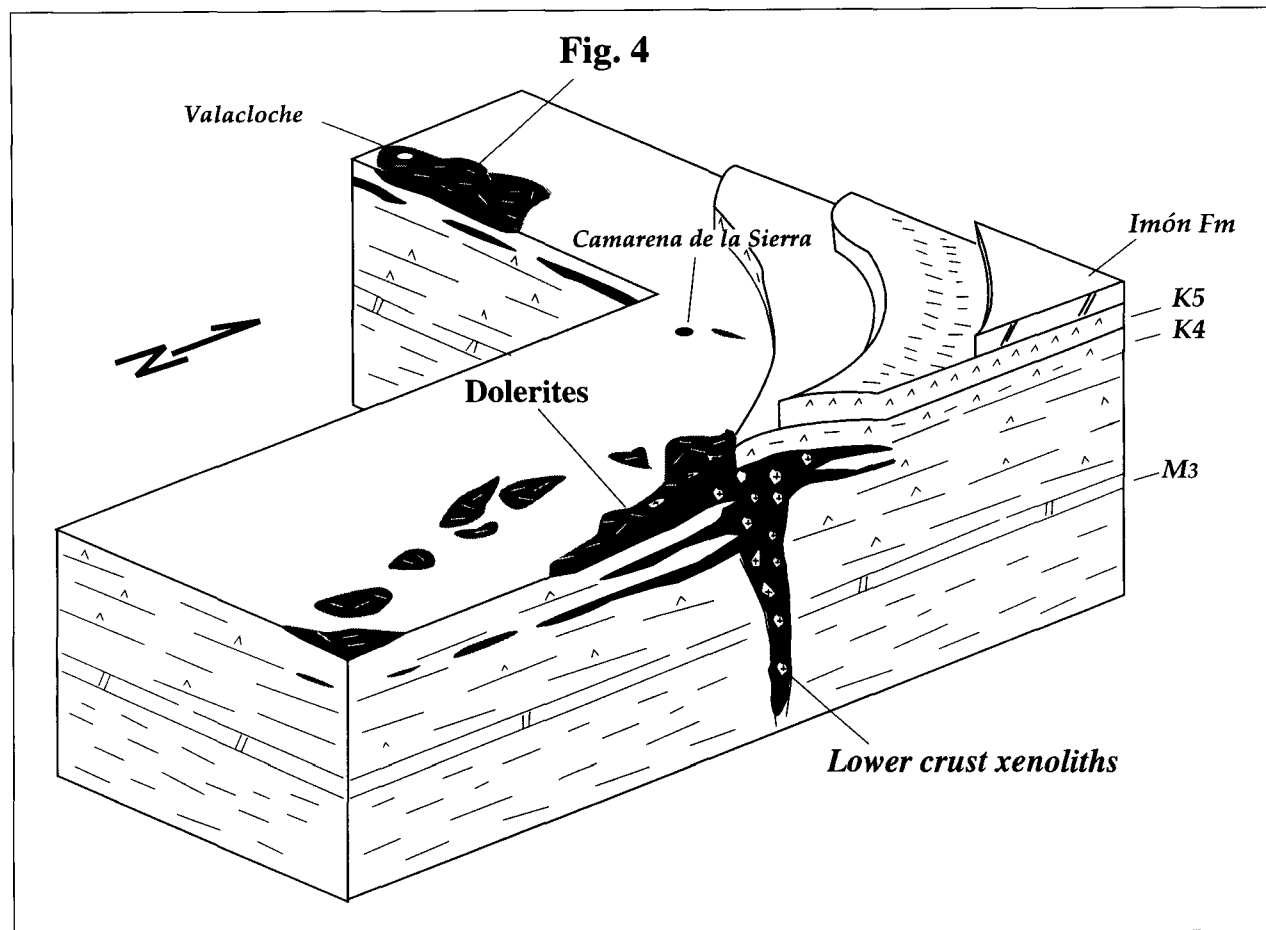
Fig. 6.—Interpretative section of dolerite emplacement, in triassic sediments, in the Valacloche and Camarena sector, showing their relationships with the host rocks and the presence of enclaves.

textures have been observed only in a few samples. The equilibrium conditions suggested for these crustal enclaves according to their mineral association (garnet + cordierite + spinel + quart + sillimanite, without orthopyroxene), must be over 900° C for the 6-9 Kb (Spear, 1993) which may correspond to a 15 km depth.

These crustal enclaves associated to the evolved liquid suggests, as previously exposed, that the ascent of the less evolved magma was favoured by pervasive fracturing of the middle-upper crust. A significant amount of magma remained in these discontinuities, reacting with some of the rock fragments (as expressed by the pyroxene rims wrapping quartzitic enclaves) and later the second, more evolved, magma batch was able to carry the enclaves together with their surrounding magma. Nevertheless, the absence of important reaction textures in enclaves points to a small-sized reservoir and a relatively fast ascent of the magma.

Petrology of the dolerites

The studied dolerites can be grouped into two rock-types: 1) Ti-augite rich dolerites and 2) differentiated dolerites, with lower modal contents of Ti-augite, but having higher biotite and potassium feldspar contents. These two rock-types have a poorly developed chilled margin facies with a quick transition to their respective central facies which are dominant in volume.

The chilled margin facies consist, for both kinds of dolerites, of scattered Ti-augite phenocrysts or glomerophyric associations, surrounded by plagioclase microlites, opaque minerals and a cryptocrystalline groundmass. Olivine (always altered) is rare and only appears in the Ti-augite rich dolerite.

The Ti-augite rich dolerite (in central facies) is predominant in the sills of Valacloche whilst it is restricted to the margins of the sills in Camarena. It has dominant doleritic and occasionally subophitic textures. The average mineral assemblage is: 50-

Table 1.—**Pyroxene composition in dolerites (1-4: Valacloche; 5-8: Camarena) and rims on quartzite enclaves in Camarena (9-12)**

Sample	1	2	3	4	5	6	7	8	9	10	11	12
SiO_2	51.12	50.02	50.74	50.14	48.65	48.24	49.78	50.10	52.66	51.49	53.27	51.92
TiO_2	1.22	2.16	2.01	1.55	2.95	3.09	1.87	1.26	0.94	0.92	0.91	1.17
Al_2O_3	2.94	4.06	2.71	2.47	4.21	4.36	3.17	2.38	1.33	1.20	1.24	1.41
V_2O_3	n.a.	n.a.	n.a.	n.a.	n.a.	n.a.	n.a.	n.a.	0.09	0.06	0.06	0.05
Cr_2O_3	0.74	0.00	0.09	0.00	0.01	0.04	0.00	0.00	0.30	0.23	0.02	0.17
Fe_2O_3	1.08	0.94	0.43	1.62	3.12	2.14	1.72	2.25	0.00	1.23	0.00	1.01
MgO	15.18	13.85	13.68	12.90	13.86	12.36	11.46	10.60	16.18	16.24	16.44	15.59
MnO	0.03	0.16	0.22	0.17	0.15	0.26	0.30	0.42	0.20	0.04	0.28	0.21
CoO	n.a.	n.a.	n.a.	n.a.	0.00	0.00	0.02	0.06	0.00	0.00	0.00	0.00
NiO	0.00	0.18	0.00	0.00	0.00	0.00	0.07	0.00	0.01	0.00	0.00	0.11
SrO	n.a.	n.a.	n.a.	n.a.	0.05	0.00	0.00	0.18	0.00	0.00	0.00	0.00
CaO	22.41	21.82	21.87	21.36	23.31	23.14	23.16	22.89	20.52	20.08	19.43	19.57
Na_2O	0.38	0.41	0.36	0.35	0.38	0.38	0.41	0.52	0.25	0.21	0.24	0.24
K_2O	0.00	0.03	0.03	0.05	0.00	0.00	0.00	0.00	0.02	0.00	0.01	0.00
FeO	4.66	6.80	8.11	9.05	4.30	6.75	8.82	9.83	6.37	6.73	8.09	8.85
Total	99.76	100.42	100.23	99.66	100.99	100.76	100.78	100.48	98.88	98.43	99.98	100.30

Number of ions on the basis of 6 O												
Si	1.89	1.85	1.89	1.89	1.83	1.82	1.89	1.92	1.96	1.95	1.96	1.94
Al_{IV}	0.11	0.15	0.11	0.11	0.17	0.18	0.11	0.08	0.04	0.05	0.04	0.06
Al_{VI}	0.02	0.03	0.01	0.00	0.01	0.02	0.03	0.03	0.02	0.00	0.02	0.00
Fe^{3+}	0.03	0.03	0.01	0.05	0.00	0.00	0.00	0.00	0.00	0.00	0.00	0.00
Ti	0.03	0.06	0.06	0.04	0.08	0.09	0.05	0.04	0.03	0.03	0.03	0.03
Cr	0.02	0.00	0.00	0.00	0.00	0.00	0.00	0.00	0.01	0.01	0.00	0.00
V	0.00	0.00	0.00	0.00	0.00	0.00	0.00	0.00	0.00	0.00	0.00	0.00
Mg	0.84	0.77	0.76	0.73	0.78	0.70	0.65	0.61	0.90	0.92	0.90	0.87
Fe^{2+} (M1)	0.06	0.12	0.16	0.18	0.13	0.20	0.27	0.33	0.05	0.05	0.05	0.09
Fe^{2+} (M2)	0.08	0.09	0.09	0.10	0.04	0.03	0.02	0.01	0.15	0.17	0.20	0.19
Mn	0.00	0.01	0.01	0.01	0.00	0.01	0.01	0.01	0.01	0.00	0.01	0.01
Ca	0.89	0.87	0.87	0.86	0.94	0.94	0.94	0.94	0.82	0.81	0.77	0.78
Na	0.03	0.03	0.03	0.03	0.03	0.03	0.03	0.04	0.02	0.02	0.02	0.02
K	0.00	0.00	0.00	0.00	0.00	0.00	0.00	0.00	0.00	0.00	0.00	0.00
Ni	n.a.	n.a.	n.a.	n.a.	0.00	0.00	0.00	0.00	0.00	0.00	0.00	0.00
Co	n.a.	n.a.	n.a.	n.a.	0.00	0.00	0.00	0.00	0.00	0.00	0.00	0.00
Sr	n.a.	n.a.	n.a.	n.a.	0.00	0.00	0.00	0.00	0.00	0.00	0.00	0.00
Total	4.0	4.0	4.0	4.0	4.0	4.0	4.0	4.0	4.0	4.0	4.0	4.0
mg^*	0.85	0.78	0.75	0.72	0.83	0.75	0.69	0.64	0.82	0.80	0.78	0.75
Wo	46.74	46.24	45.85	44.84	49.82	49.98	49.67	49.58	42.61	41.62	39.79	40.29
En	44.04	40.85	39.89	37.66	41.20	37.12	34.19	31.95	46.74	46.83	46.83	44.66
Fs	9.22	12.91	14.27	17.50	8.73	12.46	15.63	17.76	10.65	11.55	13.38	15.05

60 % augite + 35-40 % plagioclase + 3-5 % biotite + 2-3 % opaque minerals + 2 % potassium feldspar + 1 % apatite. This assemblage represents the less differentiated term of this magmatism.

The biotite rich dolerite forms the internal parts of the Valacloche sills and is the main rock-type in the central sector of the Camarena sills, where crustal enclaves occur. Doleritic texture prevails and the average mineral assemblage is: 30-35 % augite + 40-60 % plagioclase + 7-10 % biotite + 5 % potassium feldspar + 2 % quartz + 2 % opa-

que minerals + 1 % apatite ± accesory minerals (titanite).

Mineral composition

Mineral compositions were obtained with an electronic microprobe CAMECA SX-50 (Universities of Toulouse and Oviedo) operating under standard conditions (15 Kv, 10 nA, 1 μm beam diameter and 10 seconds integration time) except

Table 2.—Biotite composition (1-2: Valacloche; 3-6: Camarena and 7-10 metapelitic enclaves of Camarena)

Sample	1	2	3	4	5	6	7	8	9	10
SiO_2	37.985	38.202	34.051	36.013	34.421	33.087	33.625	33.292	33.386	33.328
TiO_2	5.318	5.282	4.793	6.235	6.628	6.214	4.087	4.102	4.028	3.923
Al_2O_3	12.077	11.838	13.465	12.664	13.249	12.695	12.897	12.676	12.846	12.941
Cr_2O_3	0.073	0.000	0.056	0.000	0.009	0.034	0.064	0.042	0.016	0.000
$FeO_{(t)}$	18.976	19.209	22.634	22.711	26.158	29.669	32.809	33.331	32.693	32.718
MnO	0.062	0.000	0.335	0.183	0.201	0.285	0.172	0.079	0.158	0.158
MgO	12.592	12.254	11.268	9.026	7.344	5.760	2.907	3.046	3.101	2.975
NiO	0.073	0.000	0.000	0.057	0.000	0.074	n.a.	n.a.	n.a.	n.a.
CaO	0.029	0.038	0.038	0.019	0.000	0.011	0.000	0.000	0.000	0.000
Na_2O	0.469	0.278	0.439	0.000	0.517	0.370	0.293	0.348	0.221	0.271
K_2O	8.869	8.749	6.015	7.841	8.688	7.837	8.489	8.460	8.348	8.332
BaO	n.a.	n.a.	n.a.	n.a.	n.a.	n.a.	0.000	0.078	0.306	0.279
Rb_2O	n.a.	n.a.	n.a.	n.a.	n.a.	n.a.	0.202	0.042	0.135	0.045
Cl	n.a.	n.a.	n.a.	n.a.	n.a.	n.a.	2.508	2.481	2.484	2.518
F	n.a.	n.a.	n.a.	n.a.	n.a.	n.a.	0.025	0.000	0.000	0.038
Total	100.26	99.95	98.52	99.26	100.38	100.24	98.05	97.98	97.72	97.49

Number of ions on the basis of 22 equivalent O										
Si	2.84	2.87	2.65	2.78	2.66	2.63	2.81	2.78	2.78	2.79
Al_{IV}	1.06	1.05	1.24	1.15	1.21	1.19	1.19	1.22	1.22	1.21
Fe^{3+}	0.00	0.00	0.00	0.00	0.00	0.00	0.00	0.00	0.00	0.00
Al_{VI}	0.00	0.00	0.00	0.00	0.00	0.00	0.08	0.02	0.05	0.06
Ti	0.30	0.30	0.28	0.36	0.39	0.37	0.26	0.26	0.25	0.25
Cr	0.00	0.00	0.00	0.00	0.00	0.00	0.00	0.00	0.00	0.00
Fe^{2+}	1.03	1.06	1.21	1.33	1.52	1.72	2.25	2.30	2.26	2.26
Mn	0.00	0.00	0.02	0.01	0.01	0.02	0.01	0.01	0.01	0.01
Mg	1.40	1.37	1.31	1.04	0.85	0.68	0.36	0.38	0.39	0.37
Ni	0.00	0.00	0.00	0.00	0.00	0.01	0.00	0.01	0.02	0.02
Ca	0.00	0.00	0.00	0.00	0.00	0.00	0.00	0.00	0.00	0.00
Na	0.07	0.04	0.07	0.00	0.08	0.06	0.05	0.06	0.04	0.04
K	0.85	0.84	0.60	0.77	0.86	0.79	0.90	0.90	0.89	0.89
Total	7.6	7.5	7.4	7.5	7.7	7.7	7.9	7.9	7.9	7.9
mg^*	0.58	0.57	0.52	0.44	0.36	0.28	0.14	0.14	0.15	0.14

for the REE analysis in apatite and titanite (20 Kv and 20 s).

Clinopyroxene is augite-diopside, displaying a Ti enrichment (table 1) from centre to border of the crystals, according with the observed optical zonation. Its Fe contents are higher in the Camarena dolerites when compared to those of Valacloche (fig. 7a). The pyroxene crystals that form the rims on quartzitic enclaves are slightly more evolved in composition than the two previous cases (fig. 7b; analysis 9 to 12 in table 1). This is coherent with their later crystallization according to the previously exposed emplacement scheme.

The high modal proportion of this mineral phase (45-60 %) allows to consider that the evolution of the liquid should be expressed in the compositional evolution of pyroxene [represented by the descent in mg^* (=$Mg/Mg+Fe^{2+}$)]. Compositions obtained on

this mineral show, from centre to border, a progressive decreasing in SiO_2 and Cr_2O_3 contents and a correlative increase in Al_2O_3, FeO and TiO_2 contents (fig. 7c). Pyroxene compositions for Camarena and Valacloche rocks are very similar for low Cr/Al ratios (fig. 7b) but in the Camarena dolerites two compositional trends can be observed; one is similar to that of Valacloche dolerites and the other is characterized by a smaller initial mg^* value. This significant difference supports an intrusive process in two different stages in the Camarena dolerites.

The pyroxene crystals forming the rims on quartzite enclaves indicate a more evolved magma compisition, with lower Cr/Al (fig. 7b) and Ti (fig. 7c) values than those analysed in dolerites; this can be explained by the fractionation of Cr and Ti in pyroxene and biotite crystals in the less evolved dolerites. Taking into account the whole available data,

Table 3.—**Plagioclase composition (1-2: Valacloche; 3-5: Camarena and 6-8: granitoid enclaves of Camarena)**

Sample	1	2	3	4	5	6	7	8
SiO_2	68.63	69.18	65.16	70.38	63.64	59.42	59.92	58.36
Al_2O_3	19.50	19.38	17.47	18.77	17.21	25.01	25.26	24.72
FeO(t)	0.00	0.31	0.12	0.13	0.03	0.17	0.06	0.51
MnO	0.05	0.03	0.06	n.a.	n.a.	n.a.	n.a.	n.a.
MgO	0.00	0.00	0.04	0.00	0.00	0.01	0.01	0.18
CaO	0.02	0.00	0.00	0.21	7.40	7.24	7.30	8.18
SrO	n.a.	n.a.	n.a.	n.a.	n.a.	0.19	0.22	0.13
Na_2O	11.75	11.80	0.27	10.47	8.41	6.60	6.75	6.37
K_2O	0.04	0.06	16.69	0.40	1.27	0.74	0.86	0.60
Rb_2O	n.a.	n.a.	n.a.	0.11	0.11	0.07	0.06	0.08
BaO	n.a.	n.a.	n.a.	n.a.	n.a.	0.23	0.17	0.00
Total	99.98	100.76	99.81	100.47	98.07	99.67	100.60	99.13

Number of ions on the basis of 32 O

	1	2	3	4	5	6	7	8
Si	3.00	3.00	3.02	3.05	2.91	2.67	2.67	2.64
Al	1.00	0.99	0.96	0.96	0.93	1.32	1.33	1.32
$Fe_{(t)}$	0.00	0.01	0.00	0.00	0.00	0.01	0.00	0.02
Mn	0.00	0.00	0.00	0.00	0.00	0.00	0.00	0.00
Mg	0.00	0.00	0.00	0.00	0.00	0.00	0.00	0.01
Ca	0.00	0.00	0.00	0.01	0.36	0.35	0.35	0.40
Na	1.00	0.99	0.02	0.00	0.00	0.57	0.58	0.56
K	0.00	0.00	0.99	0.01	0.36	0.04	0.05	0.03
Rb	0.00	0.00	0.00	0.00	0.00	0.00	0.00	0.00
Sr	0.00	0.00	0.00	0.00	0.00	0.00	0.01	0.00
Ba	0.00	0.00	0.00	0.00	0.00	0.00	0.00	0.00
Total	5.00	5.00	5.00	4.92	5.03	4.98	4.99	4.99
Or	0.20	0.34	97.60	2.40	6.26	4.41	4.96	3.51
Ab	99.70	99.66	2.40	96.51	63.10	59.52	59.51	56.45
An	0.11	0.00	0.00	1.09	30.65	36.07	35.53	40.04

the progressive Ti enrichment with nearly constant (Ca+Na) values, indicates the alkaline affinity of the liquid (Leterrier *et al.*, 1982; fig. 7c). The late pyroxene crystals in Camarena are more evolved (richer in Ti) than those analysed for the Valacloche dolerites.

Plagioclase (45-50 %) crystals are zoned and, commonly affected by secondary alteration (fig. 8; selected compositions 1 to 5 in table 3) with a high K content.

Biotite crystals are more abundant (6-7 %) in the Camarena dolerites, and have higher Fe^{2+} and Al contents (fig. 9 and selected values in table 2) than the Valacloche ones. Tiny apatite and/or Ti-magnetite inclusions are common.

Accesory minerals are Ti-magnetite (table 10), apatite (table 4), and rare titanite (table 6). Greenish amphibole is rare and probably has a subsolidus origin. A noticeable aspect of the composition of early mineral phases (apatite and titanite) is their low REE content. These elements were probably enriched in opaque minerals (not analysed).

Geochemical composition

Petrologically representative samples were analysed at the X-RAL laboratory (Toronto, Canada) by XRF (major elements and Ba, Rb, Nb, Sr and Zr), INAA (Th, Cr, Ta, Hf and U) and ICP-MS (rest of the trace elements, including REE). A selection of thirteen analysis (with LOI < 4 %), comprising the entire range of rock-types in the studied area, is given in table 11.

According to their geochemical composition, these samples are relatively evolved alkali basalts (%SiO_2 vs. Nb/Y: fig. 10a); *mg** ranges from 0.60 to 0.46 (being *mg** =Mg/Mg+Fe^{2+} and taking a 0.15 value for the Fe^{3+}/Fe^{2+} ratio). Geochemical differentiation is expressed by the gradual decrease in compatible elements (Co, Cr, V, Sc and Ni) and *mg** parameter (Cr/Ni vs. *mg**: fig. 10b). Linear-positive correlations are also observed for incompatible elements (Zr, Y, Nb, Th and Ce; g.e. La vs. Ta: fig. 10c) and ratios of strongly incompatible elements.

Table 4.—Composition of apatite crystals in dolerites

Sample	1	2	3	4	5	6
CaO	57.13	55.88	55.38	54.12	54.12	54.98
P_2O_5	41.48	41.87	41.87	41.78	42.43	40.73
La_2O_3	0.00	0.00	0.00	0.05	0.10	0.27
Ce_2O_3	0.09	0.04	0.00	0.22	0.04	0.54
Nd_2O_3	0.10	0.00	0.37	0.12	0.06	0.11
SmO	0.00	0.00	0.16	0.00	0.24	0.01
Y_2O_3	0.00	0.07	0.18	0.00	0.14	0.11
SiO_2	0.26	0.24	0.19	0.69	0.21	0.42
TiO_2	0.05	0.06	0.03	0.13	0.07	0.00
FeO	0.52	0.57	0.37	0.59	0.27	0.06
MgO	0.12	0.13	0.14	0.30	0.15	0.02
MnO	0.09	0.19	0.14	0.06	0.09	0.00
SrO	0.03	0.15	0.06	0.22	0.36	0.06
Na_2O	0.03	0.00	0.04	0.01	0.00	0.18
K_2O	0.00	0.00	0.00	0.00	0.02	0.00
BaO	0.00	0.00	0.00	0.33	0.25	0.00
F	0.61	0.84	0.56	0.50	0.94	1.53
Cl	0.15	0.13	0.16	0.13	0.12	0.42
Total	100.68	100.17	99.65	99.25	99.60	99.42

Number of ions on the basis of 26 (O, OH, F, Cl)

Ca	10.49	10.27	10.24	10.02	9.97	10.21
P	6.02	6.08	6.12	6.11	6.18	5.98
La	0.00	0.00	0.00	0.00	0.01	0.02
Ce	0.01	0.00	0.00	0.01	0.00	0.03
Nd	0.01	0.00	0.02	0.01	0.00	0.01
Sm	0.00	0.00	0.01	0.00	0.01	0.00
Y	0.00	0.01	0.02	0.00	0.01	0.01
Si	0.04	0.04	0.03	0.12	0.04	0.07
Ti	0.01	0.01	0.00	0.02	0.01	0.00
Fe	0.08	0.08	0.05	0.08	0.04	0.01
Mg	0.03	0.03	0.04	0.08	0.04	0.00
Mn	0.01	0.03	0.02	0.01	0.01	0.00
Sr	0.00	0.02	0.01	0.02	0.04	0.01
Na	0.01	0.00	0.01	0.00	0.00	0.06
K	0.00	0.00	0.00	0.00	0.00	0.00
Ba	0.00	0.00	0.00	0.02	0.02	0.00
F	0.33	0.46	0.30	0.27	0.51	0.84
Cl	0.04	0.04	0.05	0.04	0.03	0.12
Total	17.1	17.1	16.9	16.8	16.9	17.4

Table 5.—Composition of amphibole in a metapelitic enclave

Sample	1	2	3	4	5
SiO_2	50.034	50.393	53.414	53.283	52.062
TiO_2	0.103	0.122	0.177	0.177	0.012
Al_2O_3	3.341	3.575	1.889	2.046	2.400
V_2O_3	0.000	0.084	0.028	0.000	0.000
Cr_2O_3	0.000	0.000	0.000	0.000	0.069
FeO	16.547	16.553	12.535	14.044	16.358
MgO	13.318	13.235	15.818	15.155	13.717
MnO	0.031	0.143	0.124	0.072	0.071
NiO	0.024	0.000	0.031	0.000	0.032
CaO	11.720	11.777	12.118	11.903	11.998
Na_2O	0.755	0.741	0.596	0.643	0.497
K_2O	0.332	0.331	0.157	0.117	0.212
BaO	0.000	0.000	0.291	0.000	0.041
Cl	0.084	0.095	0.000	0.002	0.038
F	0.054	0.000	0.000	0.016	0.000
Total	96.34	97.05	97.18	97.46	97.51

Number of ions on the basis of 24 equivalent O

Si	7.445	7.442	7.736	7.710	7.624
Al_{IV}	0.555	0.558	0.264	0.290	0.376
Al_{VI}	0.031	0.065	0.059	0.059	0.038
Ti	0.012	0.014	0.019	0.019	0.001
Cr	0.000	0.000	0.000	0.000	0.008
Fe^{3+}	0.178	0.164	0.053	0.096	0.132
Mg	2.954	2.913	3.415	3.268	2.994
Fe^{2+}_C	1.825	1.845	1.454	1.558	1.827
Fe^{2+}_B	0.056	0.036	0.011	0.046	0.044
Mn	0.004	0.018	0.015	0.009	0.009
Ni	0.003	0.000	0.004	0.000	0.004
V	0.000	0.015	0.005	0.000	0.000
Ca	1.869	1.863	1.881	1.845	1.882
Na_B	0.069	0.068	0.084	0.090	0.061
Na_A	0.040	0.038	0.000	0.000	0.010
K	0.032	0.031	0.015	0.011	0.020
Ba	0.000	0.000	0.017	0.000	0.002
Total	15.1	15.1	15.0	15.0	15.0
mg^*	0.61	0.61	0.70	0.67	0.62

The alkaline affinity is expressed in high values for the total alkalies ($Na_2O + K_2O = 6.2$ % on average), high TiO_2 contents (ranging 2.1-2.7 %), high Ti/V ratio (Shervais, 1982; fig. 10d), a high content in P_2O_5 (0.63 % on average) and also some high values for Nb and Ta, with averages in 48 and 3 ppm respectively; this alkaline affinity is in agreement with the interelemental ratios shown in table 11.

An OIB-normalized (Sun & McDonough, 1989; fig. 11a) spider diagram shows positive anomalies for K and P and a significant Sr depletion (correlative with U and Th negative anomalies) for most of the samples (table 11). These low Sr contents are in

agreement with low modal proportions of calcic plagioclase in the rocks.

The observed patterns both in normalized spider (fig. 11a) and REE (fig. 11b) plots indicate the close similarity of the studied rocks with a typical OIB pattern. This similarity is also expressed by other trace elements [Ti, V (fig. 10d), Nb and Ta] which also confirm the alkaline affinity. Camarena dolerites have more evolved geochemical compositions, when compared with those of Valacloche. Fractionation is related to variations in the modal proportions of augite (which preferently concentrates Cr, with respect to Ni and the rest of the compatible elements), plagioclase (with increasing Sr, Ba contents and Eu positive anomaly as the composition evolves) and biotite

Table 6.—Sphene (titanite) composition in a metapelitic enclave

Sample	1	2	3	4	5	6
SiO_2	29.768	29.636	29.674	29.820	30.680	29.787
TiO_2	37.560	37.175	37.178	37.335	37.330	37.452
ZrO_2	0.462	0.863	0.269	0.782	0.459	1.033
Nb_2O_3	0.137	0.000	0.000	0.000	0.179	0.091
Ta_2O_5	0.000	0.000	0.000	0.000	0.000	0.000
Y_2O_3	0.000	0.164	0.212	0.000	0.000	0.376
Al_2O_3	0.688	0.673	0.788	0.682	0.671	0.678
Cr_2O_3	0.000	0.000	0.000	0.018	0.000	0.000
FeO	1.971	1.976	2.004	1.923	1.811	2.182
MnO	0.045	0.000	0.040	0.025	0.084	0.049
MgO	0.027	0.000	0.013	0.000	0.020	0.008
CaO	31.879	31.477	31.647	31.280	31.598	30.912
SrO	0.000	0.031	0.000	0.000	0.101	0.000
Na_2O	0.018	0.018	0.012	0.024	0.039	0.019
K_2O	0.000	0.013	0.000	0.000	0.000	0.000
F	0.011	0.011	0.211	0.000	0.022	0.100
Total	102.57	102.04	102.05	101.89	102.99	102.69

Number of ions on the basis of 1 Si						
Si	1.000	1.000	1.000	1.000	1.000	1.000
Ti	0.949	0.943	0.942	0.942	0.915	0.946
Al	0.027	0.027	0.031	0.027	0.026	0.027
Fe^{3+}	0.055	0.056	0.056	0.054	0.049	0.061
Mg	0.001	0.000	0.001	0.000	0.001	0.000
Zr	0.008	0.014	0.004	0.013	0.007	0.017
Cr	0.000	0.000	0.000	0.000	0.000	0.000
Nb	0.002	0.000	0.000	0.000	0.003	0.001
Ta	0.000	0.000	0.000	0.000	0.000	0.000
Σ O	1.010	1.009	1.007	1.010	0.992	1.022
Ca	1.147	1.138	1.143	1.124	1.103	1.112
Na	0.001	0.001	0.001	0.002	0.002	0.001
Mn	0.001	0.000	0.001	0.001	0.002	0.001
Sr	0.000	0.001	0.000	0.000	0.002	0.000
Y	0.000	0.003	0.004	0.000	0.000	0.007
Σ M	1.150	1.143	1.148	1.126	1.110	1.121
Total	5.16	5.16	5.15	5.13	5.05	5.16

Table 7.—Spinel composition in a metapelitic enclave

Sample	1	2	3	4	5	6
SiO_2	0.09	0.12	0.06	0.09	0.06	0.10
TiO_2	0.51	0.57	0.53	0.58	0.57	0.64
Al_2O_3	59.28	59.44	59.38	59.57	59.53	59.13
V_2O_3	0.28	0.07	0.22	0.12	0.09	0.06
Cr_2O_3	0.14	0.11	0.09	0.11	0.25	0.16
Fe_2O_3	2.19	2.09	2.67	2.54	2.15	2.78
MgO	7.94	8.04	8.16	8.08	8.05	7.80
CaO	0.01	0.00	0.00	0.00	0.00	0.00
MnO	0.11	0.29	0.33	0.12	0.14	0.17
FeO	28.91	28.53	28.40	28.35	28.62	28.83
CoO	0.00	0.01	0.00	0.09	0.10	0.15
NiO	0.00	0.00	0.00	0.05	0.00	0.08
ZnO	0.06	0.06	0.17	0.49	0.19	0.24
Na_2O	0.00	0.01	0.01	0.04	0.00	0.02
Total	99.52	99.33	100.01	100.23	99.73	100.14

Number of ions on the basis of 32 O						
Si	0.02	0.03	0.01	0.02	0.01	0.02
Ti	0.08	0.09	0.09	0.10	0.09	0.11
Al	15.43	15.47	15.38	15.40	15.45	15.34
V	0.05	0.01	0.04	0.02	0.02	0.01
Cr	0.02	0.02	0.01	0.02	0.04	0.03
Fe^{3+}	0.36	0.35	0.44	0.42	0.36	0.46
Fe^{2+}	5.34	5.27	5.22	5.20	5.27	5.31
Mg	2.61	2.65	2.67	2.64	2.64	2.56
Mn	0.02	0.05	0.06	0.02	0.03	0.03
Co	0.00	0.00	0.00	0.02	0.02	0.03
Ni	0.00	0.00	0.00	0.01	0.00	0.01
Zn	0.01	0.01	0.03	0.08	0.03	0.04
Ca	0.00	0.00	0.00	0.00	0.00	0.00
Na	0.00	0.00	0.01	0.02	0.00	0.01
Total	24.0	24.0	24.0	24.0	24.0	24.0
mg*	0.31	0.32	0.32	0.32	0.32	0.31

(increase of the Rb, Ba and Nb contents). The high TiO_2 contents agree with the progressive Ti enrichment in augite (and titanite) and the common apatite crystals justify the P_2O_5 contents.

When comparing these alkaline dolerites of the SE of the Iberian Chain with the tholeiitic ones of the southern sector of Valencia (Lago et al., 1999) —both with pre-Hettangian age and a pre-Liassic rifting related emplacement—, the alkaline dolerites considered in this study define a Ti and P-rich domain (High Titanium Basalts or HTB). This alkaline domain, as shown by incompatible element ratios (Th/Ta vs. Th/Tb; fig. 12) and REE contents, is clearly different from that defined by the tholeiitic dolerites of the SE margin of the Iberian Chain (Valencia; Lago et al., 1999), which were probably geodynamically related to a pre-Betic rifting (Lago et al., 1999). These two domains (alkaline and tholeiitic) could be the result of different distension rates affecting the Iberian crust or even the petrological expression of differences in thicknes of the overlying crust.

Discussion

The triassic dolerites of the Valacloche and Camarena sectors (SE of the Iberian Chain) have an alkaline affinity (expressed in their modal, mineral and geochemical compositions) and a moderate fractionation. This fractionation results in two dolerite types (with different modal percentages in Ti-augite and biotite), represented in the two studied outcrops, and accompanied, in the Camarena intrusion by a enclave-rich unit. These field relations-

Table 8.—Sillimanite composition in a metapelitic enclave.

Sample	1	2	3	4	5	6
SiO_2	37.012	36.883	37.081	37.015	36.861	37.089
Al_2O_3	62.082	62.144	62.262	62.565	62.529	62.165
TiO_2	0.000	0.000	0.056	0.015	0.014	0.000
Cr_2O_3	0.096	0.120	0.168	0.012	0.108	0.084
FeO	0.212	0.086	0.162	0.311	0.243	0.167
MnO	0.073	0.000	0.000	0.031	0.000	0.063
MgO	0.000	0.010	0.000	0.015	0.007	0.000
NiO	0.031	0.000	0.000	0.000	0.000	0.000
Cao	0.000	0.000	0.000	0.012	0.041	0.000
Na_2O	0.008	0.001	0.021	0.000	0.000	0.005
Total	99.51	99.24	99.75	99.98	99.80	99.57

Number of ions on the basis of 20 Oxygens						
Si	4.020	4.012	4.016	4.002	3.992	4.023
Al_{IV}	3.980	3.988	3.984	3.998	4.008	3.977
Al_{VI}	3.966	3.979	3.964	3.974	3.973	3.971
Ti	0.000	0.000	0.005	0.001	0.001	0.000
Cr	0.008	0.010	0.014	0.001	0.009	0.007
Fe^{3+}	0.019	0.008	0.015	0.028	0.022	0.015
Mn	0.007	0.000	0.000	0.003	0.000	0.006
Mg	0.000	0.002	0.000	0.002	0.001	0.000
Ni	0.003	0.000	0.000	0.000	0.000	0.000
Ca	0.000	0.000	0.000	0.001	0.005	0.000
Na	0.000	0.000	0.001	0.000	0.000	0.000
Total	12.0	12.0	12.0	12.0	12.0	12.0

Table 9.—Cordierite composition in a metapelitic enclave.

Sample	1	2	3	4	5
SiO_2	47.445	47.178	47.002	47.165	47.040
TiO_2	0.120	0.147	0.107	0.103	0.143
Al_2O_3	32.104	33.036	32.748	32.765	32.473
MgO	8.086	8.177	8.051	7.725	7.488
CaO	0.026	0.021	0.046	0.011	0.058
MnO	0.124	0.176	0.176	0.041	0.207
FeO	8.877	9.349	9.525	10.015	10.155
Na_2O	0.193	0.177	0.254	0.205	0.178
K_2O	0.476	0.659	0.517	0.452	0.490
Total	97.451	98.920	98.426	98.482	98.232

Number of ions on the basis of 18 Oxygens					
Si	4.97	4.89	4.90	4.91	4.92
Al_{IV}	1.03	1.11	1.10	1.09	1.08
Al_{VI}	2.93	2.92	2.92	2.93	2.92
Ti	0.01	0.01	0.01	0.01	0.01
Mg	1.26	1.26	1.25	1.20	1.17
Fe	0.78	0.81	0.83	0.87	0.89
Mn	0.01	0.02	0.02	0.00	0.02
Ca	0.00	0.00	0.01	0.00	0.01
Na	0.04	0.04	0.05	0.04	0.04
K	0.06	0.09	0.07	0.06	0.07
Total	11.1	11.1	11.1	11.1	11.1
mg^*	0.62	0.61	0.60	0.58	0.57

hips, together with structural constraints strongly suggest a main magma ascent conduit, related to the intrusion to the S of Camarena (fig. 6). The intruding magma was emplaced concordantly with the bedding planes, in the form of sheet-like injections in the Camarena outcrop or as individualized sills in the case of Valacloche. In both cases, fluidality structures and very low grade contact metamorphism, were favoured by the plastic character of damp sediments in Keuper facies prior to the dolomitic sedimentation of the Imón Fm. In these subvolcanic conditions and with an adequate stratigraphic control the magma could reach a wide lateral extension; the relative vicinity of doleritic sills suggests an initially reduced number of intrusions.

Crustal enclaves (quartzites, granitoids and high grade metapelites) are associated to the most evolved dolerite and occur in the internal part of the Camarena outcrop. The magmatic conduits were probably developed by pervasive fracturing, related to the onset of the Triassic rifting events, of the middle and upper crust, as the enclaves derive from different levels of the crust. Magma ascent probably took place in two successive stages. The first, corresponding to an unevolved basaltic magma is represented by the less evolved

Table 10.—Composition of opaque minerals in dolerites.

Sample	1	2	3	4	5
TiO_2	53.782	53.764	53.795	53.720	53.922
FeO	46.659	46.471	46.963	46.713	46.917
Cr_2O_3	0.042	0.083	0.073	0.020	0.000
MnO	0.910	0.928	0.785	0.833	1.051
Total	101.39	101.25	101.62	101.29	101.89

Number of ions on the basis of 6 Oxygens					
Ti	2.010	2.011	2.007	2.010	2.007
Fe^{3+}	0.000	0.000	0.000	0.000	0.000
Cr	0.002	0.003	0.003	0.001	0.000
Fe^{2+}	1.939	1.933	1.949	1.944	1.942
Mn	0.038	0.039	0.033	0.035	0.044
Total	4.0	4.0	4.0	4.0	4.0

dolerites and indicates the fast ascent of the magma with short residence time in the reservoir. A more differentiated magma, with a longer residence time in the reservoir and in contact with the enclaves, was extruded later, forming the second stage. Finally, ascent of the residual, more viscous magma, carrying the enclaves, completed the

a)

Ca

50

45

Diopside

20   Augite

Mg   → Fe

◇ Camarena
+ Valacloche
○ Xenoliths

b)

Cr/Al

◇ Valacloche
+ Camarena
○ Xenoliths

0.30
0.20
0.10
0.00

1.00   0.90   0.80   0.70   0.60

mg*

c)

Ti (in formula)

◇ Valacloche
+ Camarena
○ Xenoliths

0.16
0.12
0.08
0.04
0.00

A

S

0.00   0.40   0.80   1.20   1.60   2.00
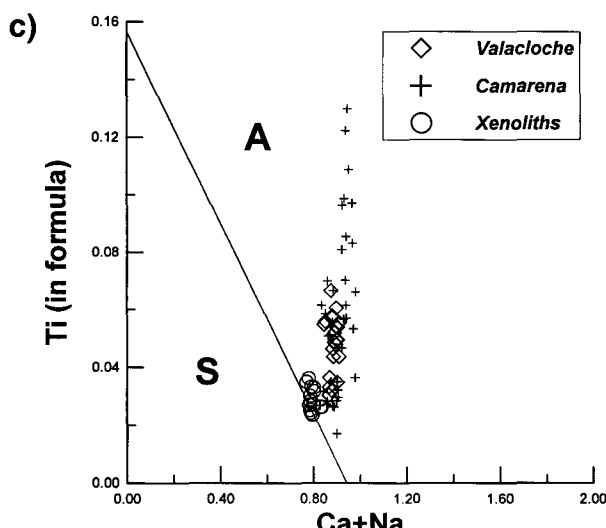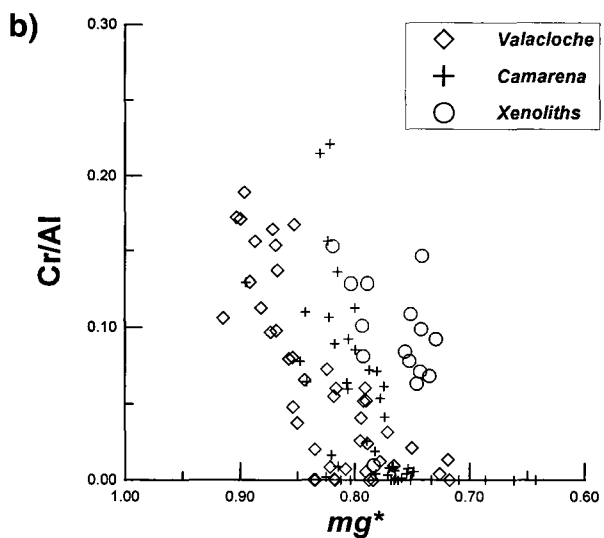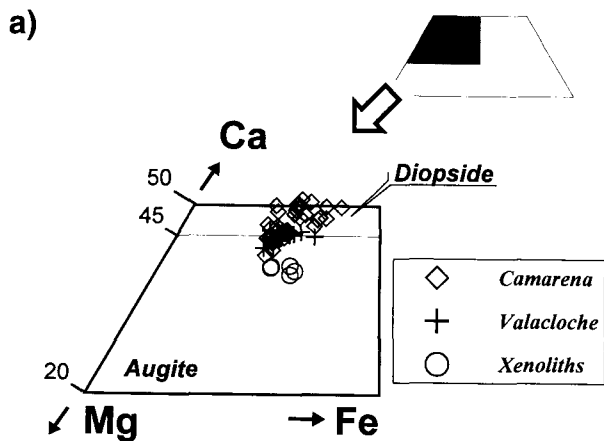
Ca+Na

Fig. 7.—In (a): clinopyroxene compositions (Morimoto *et al.*, 1988) in Valacloche and Camarena rocks and in the rims on quartzite enclaves from Camarena. (b): Cr/Al *vs.* *mg** plot and (c): Ti *vs.* (Ca+Na) plot (Leterrier *et al.*, 1982).

Or

◇ Valacloche
+ Camarena

25   75

50   50

75   25

Ab   25   50   75   An

Fig. 8.—Plagioclase composition.

0.80

◇ Valacloche
+ Camarena

Fe / (Fe+Mg)

0.60

0.40   **Biotite**

Phlogopite

0.20
0.80   1.00   1.20   1.40

Al (IV)
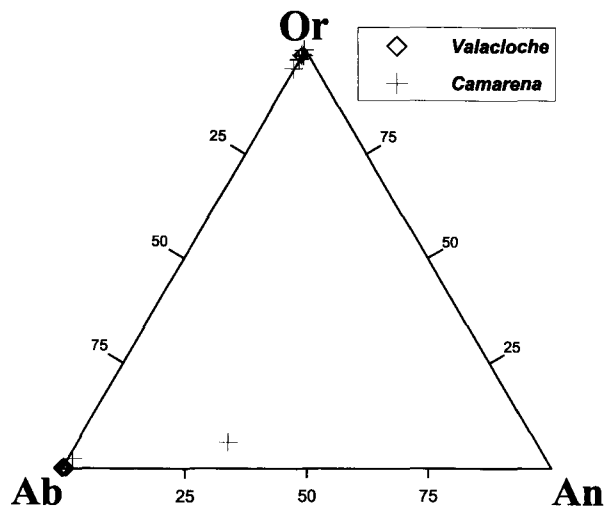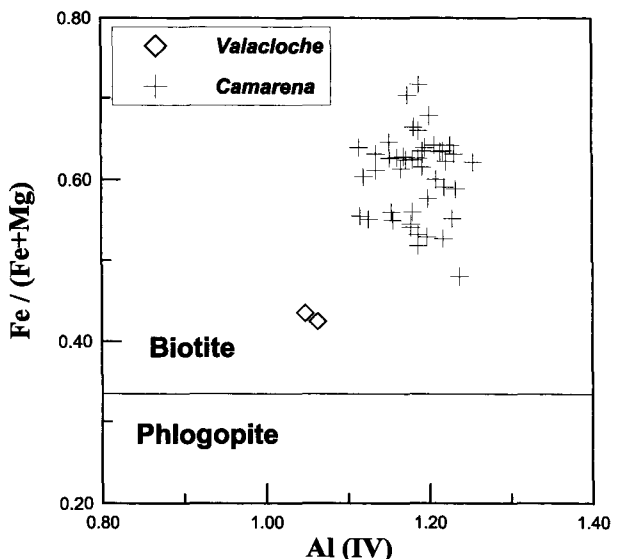
Fig. 9.—Biotite composition.

intrusive sequence. These dolerites are the first magmatic expression of the Triassic rifting that affected the Iberian Chain, which has been proposed in other studies.

The sedimentary and structural evolution of the Triassic sedimentary basins in the SE sector of the Iberian Chain, have been related to the process of triassic rifting that began in the Upper Permian and lasted until the Hettangian, and was the main external control on their sedimentary infill (Salas & Casas, 1993). In this context the beginning of the rifting stages was related to the late-variscan fracturation, which was responsible for the genesis of

Table 11.—Geochemical composition of dolerites and trace element ratios (1-6: Valacloche; 7-13: Camarena)

| Sample	1	2	3	4	5	6	7	8	9	10	12	13
SiO$_2$	50.10	51.20	48.10	49.30	49.90	49.80	47.10	47.10	49.10	46.10	48.20	47.50
TiO$_2$	2.71	2.68	2.49	2.36	2.30	2.47	2.64	2.62	2.35	2.73	2.58	2.83
Al$_2$O$_3$	15.20	15.00	13.60	13.90	12.70	13.10	13.50	14.00	12.30	14.70	14.80	14.80
Fe$_2$O$_3$	10.90	10.00	12.10	10.50	11.10	11.20	11.40	11.20	10.50	12.80	11.40	11.80
MnO	0.23	0.14	0.27	0.12	0.16	0.20	0.20	0.23	0.14	0.13	0.21	0.18
MgO	4.02	4.31	7.65	5.46	6.84	6.03	5.78	5.41	6.87	5.00	4.69	4.41
CaO	5.02	6.85	4.95	8.33	8.59	7.91	9.85	8.51	9.41	5.06	8.47	9.44
Na$_2$O	2.84	3.35	3.01	3.16	3.24	2.56	2.39	2.09	3.81	3.56	2.70	3.09
K$_2$O	5.63	3.64	3.76	2.83	2.37	4.15	3.19	4.60	1.00	3.08	3.97	2.52
P$_2$O$_5$	0.71	0.74	0.58	0.59	0.48	0.51	0.66	0.66	0.47	0.87	0.70	0.81
L.O.I.	2.28	2.40	3.60	2.60	2.35	2.15	2.65	2.75	2.45	4.00	2.50	2.95
*mg**	0.46	0.50	0.59	0.54	0.58	0.55	0.54	0.52	0.60	0.47	0.48	0.46
Total	99.80	100.40	100.20	99.20	100.10	100.20	99.40	99.30	98.40	98.10	100.40	100.40
Li	55.00	47.00	42.00	39.00	44.00	28.00	21.00	34.00	19.00	185.00	28.00	24.00
Sc	10.00	11.00	13.00	14.00	24.00	19.00	15.00	16.00	25.00	9.00	13.00	12.00
V	158.00	163.00	154.00	182.00	201.00	204.00	190.00	213.00	214.00	101.00	173.00	185.00
Cr	49.00	44.00	140.00	130.00	300.00	260.00	100.00	74.00	430.00	30.00	76.00	63.00
Co	21.00	20.00	34.00	25.00	29.00	29.00	26.00	27.00	30.00	24.00	22.00	24.00
Ni	12.00	12.00	116.00	38.00	48.00	35.00	46.00	39.00	53.00	9.00	25.00	23.00
Cu	26.10	6.80	20.50	12.40	12.10	33.40	39.40	34.10	13.30	39.00	32.90	35.20
Zn	138.00	126.00	45.30	29.20	161.00	186.00	129.00	114.00	53.30	155.00	129.00	147.00
Rb	65.00	35.00	50.00	34.00	22.00	46.00	51.00	69.00	17.00	36.00	57.00	38.00
Sr	540.00	236.00	595.00	248.00	163.00	224.00	396.00	660.00	174.00	262.00	546.00	339.00
Y	21.00	24.00	18.00	20.00	20.00	19.00	22.00	24.00	19.00	25.00	23.00	24.00
Zr	231.00	200.00	201.00	190.00	153.00	167.00	218.00	259.00	177.00	228.00	255.00	234.00
Nb	53.00	44.00	43.00	47.00	31.00	37.00	54.00	58.00	36.00	59.00	61.00	59.00
Ba	906.00	394.00	557.00	426.00	290.00	546.00	391.00	803.00	180.00	374.00	657.00	290.00
La	30.90	29.70	27.70	26.00	19.50	22.20	34.30	38.20	21.80	43.60	38.30	37.90
Ce	61.30	61.80	51.60	51.70	41.20	44.70	65.60	72.40	45.00	82.10	72.80	73.40
Pr	7.20	7.50	6.00	6.10	5.20	5.30	7.60	8.10	5.60	9.20	8.00	8.30
Nd	30.50	32.30	25.70	25.50	23.50	22.90	31.90	32.90	24.40	38.40	32.40	34.20
Sm	7.60	8.20	6.50	6.50	6.40	6.10	7.80	8.10	6.20	8.70	7.70	8.20
Eu	2.53	2.48	2.14	2.04	2.14	2.12	2.49	2.57	1.95	3.03	2.41	2.53
Gd	6.90	7.30	6.00	6.10	6.00	5.70	7.20	7.60	5.90	8.50	7.10	7.50
Tb	0.90	1.00	0.80	0.80	0.80	0.70	1.00	1.00	0.80	1.10	0.90	1.00
Dy	4.70	5.10	4.30	4.30	4.40	4.00	5.10	5.10	4.50	5.80	4.90	5.10
Ho	0.77	0.86	0.71	0.70	0.74	0.64	0.83	0.84	0.74	0.95	0.80	0.84
Er	1.90	2.10	1.80	1.80	1.80	1.60	2.10	2.10	1.90	2.50	2.00	2.10
Yb	1.50	1.60	1.20	1.40	1.40	1.20	1.50	1.60	1.40	1.80	1.50	1.50
Lu	0.19	0.20	0.15	0.18	0.17	0.15	0.21	0.20	0.18	0.24	0.20	0.20
Hf	5.30	5.10	4.50	4.40	4.00	4.40	5.00	5.90	6.10	6.60	6.20	6.10
Ta	3.40	3.60	3.10	2.70	2.60	2.30	4.00	3.70	2.80	2.20	4.20	4.70
Th	5.00	4.60	4.00	4.20	3.30	3.60	5.20	6.30	4.40	5.20	6.50	6.00
U	2.50	2.00	1.70	1.30	1.30	1.00	2.10	2.10	0.70	1.40	3.00	2.50
Nb/Y	2.52	1.83	2.39	2.35	1.55	1.95	2.45	2.42	1.89	2.36	2.65	2.46
La/Ce	0.50	0.48	0.54	0.50	0.47	0.50	0.52	0.53	0.48	0.53	0.53	0.52
La/Nb	0.58	0.68	0.64	0.55	0.63	0.60	0.64	0.66	0.61	0.74	0.63	0.64
Nb/Ta	15.59	12.22	13.87	17.41	11.92	16.09	13.50	15.68	12.86	26.82	14.52	12.55
Th/Ta	1.47	1.28	1.29	1.56	1.27	1.57	1.30	1.70	1.57	2.36	1.55	1.28
Th/Tb	5.56	4.60	5.00	5.25	4.13	5.14	5.20	6.30	5.50	4.73	7.22	6.00
Zr/Y	11.00	8.33	11.17	9.50	7.65	8.79	9.91	10.79	9.32	9.12	11.09	9.75
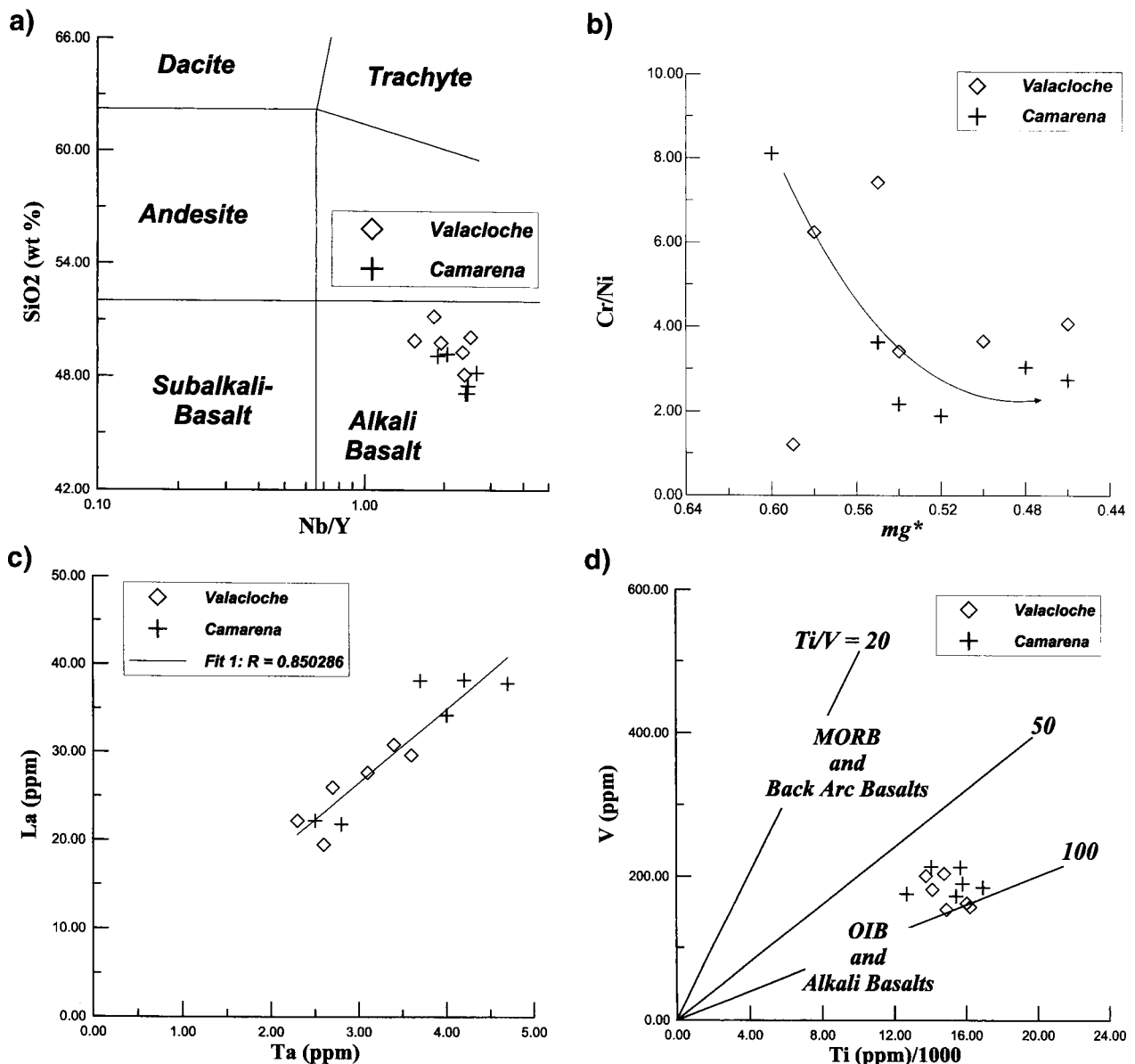
Fig. 10.—In (a): geochemical composition in the SiO_2 vs. Nb/Y (Winchester & Floyd, 1977) plot; (b): Cr/Ni vs. mg* plot; (c): La vs. Ta plot and (d): V vs. Ti/1000 plot (Shervais, 1982).

subsident basins, that progressed with a constant tectonic subsidence rate until the end of the deposit of the Triassic supersequence (Salas & Casas, 1993). The progress of this Triassic rifting at a crustal scale is consistent with the emplacement of this magmatism, rich in crustal enclaves, in the highest levels of the upper Triassic sequence. The alkaline affinity of the studied rocks, close to an OIB geochemical signature, is compatible with the early stages of a passive rifting model, under a slightly distensive regime affecting the crust and accordingly, a low partial melting ratio of the underlaying mantle.

This magmatic activity was continued, as the rifting progressed, by another alkaline magmatism emplaced within Liassic sediments of the SE of the Iberian Chain (from Cubla to Segorbe fig. 1B; Martínez et al., 1998).

Conclusions

The dolerite sills of the Valacloche-Camarena sector (SE Iberian Chain) are emplaced within the Triassic sediments of Keuper facies. The reduced
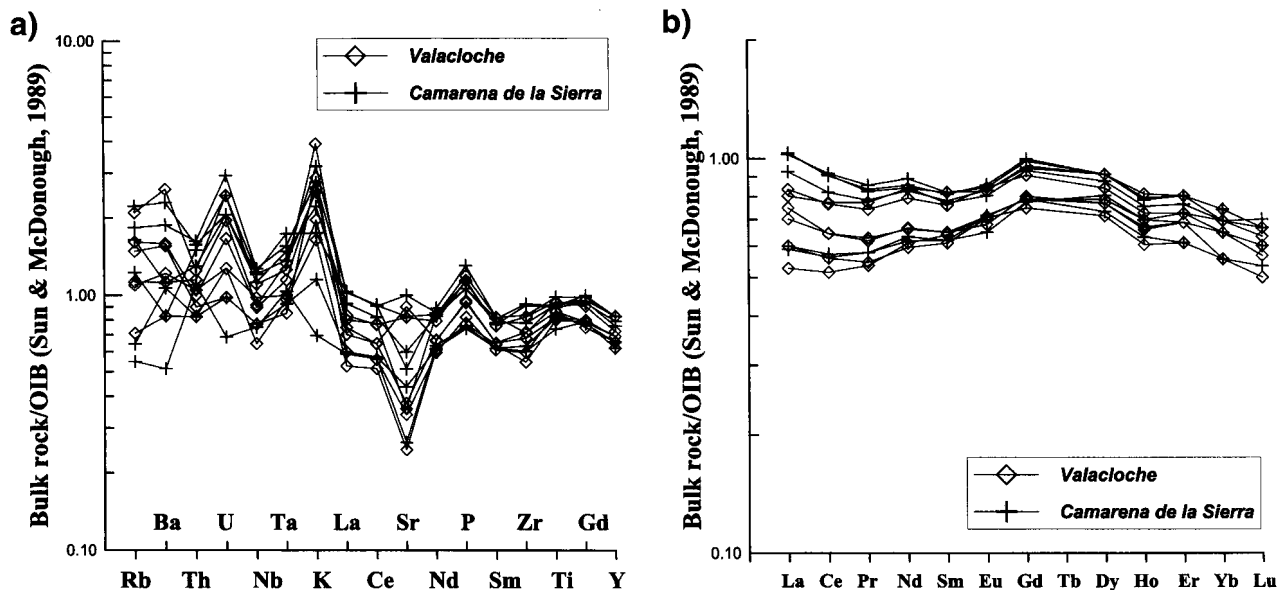
Fig. 11.—OIB-normalized plots: (a): spider-diagram and (b): REE patterns.
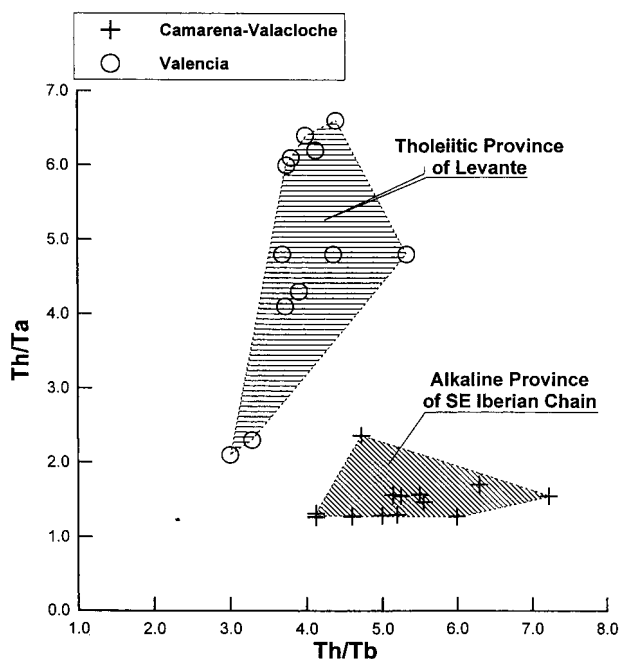
Fig. 12.—Th/Ta vs. Th/Tb plot of triassic alkaline dolerites, compared with the tholeiitic ones of Valencia (Lago et al., 1999).

lithostatic pressure and the poorly lithified character of these sediments favoured a wide areal spreading of the intrusions. In some cases, these emplacement conditions allowed for the development of fluidality structures at the top of the sills. Very low grade contact metamorphism, affecting a thin sheet of the

host sediments is common in all of the studied outcrops.

The alkaline affinity of these dolerites is supported by its mineral assemblage (Ti-augite and a variable content in accessory minerals such as apatite and titanite) and its geochemical composition (high Nb, P, and Y contents and moderate Ta contents). Spider diagram plots and REE patterns show close similarities with the composition of OIB-type basalts.

Fractionation is expressed in two rock-types (with different Ti-augite modal proportions) and is verified by the whole rock geochemical composition of these rocks (incompatible elements concentrations and normalized REE trends), as well as for the Ti-augite compositional variation.

Crustal enclaves are common, prevailing upper crust compositions over those of middle crust (high grade metapelites and granitoids). Enclave-magma reaction textures are not common which indicates a relatively quick magma ascent. The absence of higher grade metamorphic enclaves indicates a more effective fracturation at upper-middle crustal levels.

This magmatism was emplaced prior to the Hettangian, being the first expression of the Triassic rifting in this part of the Iberian Chain. This rifting was characterized by the development of subsident basins at upper crustal levels and by an increasing distension rate from the Permian to the end of the Triassic at deeper levels (Salas & Casas, 1993). Under these conditions, the reduced distension is represented by this alkaline magmatism, similar in

composition to the OIB type. Finally, the continuity of the distension regime is expressed by the later liassic magmatism emplaced in the near sectors of Cubla and Segorbe (Martínez *et al.*, 1997).

References

Goy, A. and Yébenes, A. (1977). Características, extensión y edad de la formación dolomías tableadas de Imón. *Cuad. Geol. Ibérica*, 4: 375-384.

Lago, M., Dumitrescu, R., Bastida, J., Arranz, E., Gil, A., Pocovi, A., Lapuente, M. P. and Vaquer, R. (1996). Características de los magmatismos alcalino y subalcalino, pre-Hettangiense, del borde SE de la Cordillera Ibérica. *Cuad. Geol. Ibérica*, 20: 159-181.

Lago, M., Arranz, E., Galé, C. and Bastida, C. (1999). Las doleritas toleíticas triásicas del sector SE de la Cordillera Ibérica: petrología y geoquímica. *Estudios Geol.*, 55, 5-6: 223-235.

Leterrier, J., Maury, R. C., Thonon, P., Girard, D. and Marchal, M. (1982). Clinopyroxene composition as a method of identification of the magmatic affinities of paleovolcanic series. *Earth Planet. Sci. Letters*, 59: 139-154.

Martínez, R., Lago, M., Valenzuela, J. I., Vaquer, R., Salas, R. and Dumitrescu, R. (1997). El vulcanismo triásico y jurásico del sector SE de la Cadena Ibérica y su relación con los estadios de rift mesozoicos. *Bol. Geol. Min.*, 108: 367-376.

Morimoto, N., Fabriés, J., Ferguson, A. K., Ginzburg, I. V., Ross, M., Seifert, F. A., Zussman, J., Aoki, K. and

Gottardi, G. (1988). Nomenclature of pyroxenes. *Amer. Mineral.*, 173: 1123-1133.

Orti, F. (1990). Introducción al Triásico evaporítico del sector central valenciano. In: *Formaciones evaporíticas de la Cuenca del Ebro y cadenas periféricas, y de la zona de Levante* (F. Ortí and J. M. Salvany, edits.). ENRESA-Univ. Barcelona: 205-211.

Salas, R. and Casas, A. (1993). Mesozoic extensional tectonics, stratigraphy and crustal evolution during the Alpine cycle of the eastern Iberian basin. *Tectonophysics*, 228: 33-55.

Sánchez Cela, V. (1981). Sillimanite-bearing rocks of alpine age associated to triassic materials near Teruel (Spain). *Estudios Geol.*, 37: 135-140.

Sánchez Cela, V. (1982). On the existence of hornfels associated to Triassic materials of Keuper facies, near Teruel (Spain). *Estudios Geol.*, 38: 405-413.

Sánchez Cela, V. and García, J. A. (1984). Igneous rocks of alpine age associated with Keuper materials in the Iberian mountains, near Teruel (Spain). *Estudios Geol.*, 40: 23-32.

Sánchez Cela, Auqué, L. and Fernández, J. (1987-1988). Hight T-P minerals associated with fracture-shear zones in alpine materials (Camarena, Teruel, Spain). *Rev. Inv. Geol.*, 44/45: 113-126.

Shervais, J. W. (1982). Ti-V plots and the petrogenesis of modern and ophiolitic lavas *Earth Planet. Sci. Letters*, 59: 101-118.

Spear, F. S. (1993). *Metamorphic phase equilibria and pressure-temperature-time paths.* Miner. Soc. America, Washington, 799 págs.

Sun, S. S. and McDonough, W. F. (1989). Chemical and isotopic systematics of oceanic basalts: implications for mantle composition and processes. In: *Magmatism in ocean basins* (A. D. Saunders and M. J. Norry, edits.). Geol. Soc. London. Spec. Pub. 42: 313-345.

Winchester, J. A. and Floyd, P. A. (1976). Geochemical magma type discrimination: application to altered and metamorphosed basic igneous rocks. *Earth Planet. Sci. Letters*, 28: 459-469.